231090

UCRL-JC-126828
PREPRINT

Concept for High-Charge-State Ion Induction Accelerators

B. G. Logan, M. D. Perry,
and G. J. Caporaso

This paper was prepared for submittal to
International Atomic Energy Agency Technical Committee
Meeting on Drivers and Ignition Facilities for Inertial Fusion
Osaka, Japan
March 10-14, 1997

November 15, 1996

Lawrence Livermore National Laboratory

Concept for High-Charge-State Ion Induction Accelerators

B. Grant Logan, Michael D. Perry, and George J. Caporaso
Lawrence Livermore National Laboratory *
L-481 Livermore, California, USA, 94550
IAEA TCM on Drivers and Ignition Facilities for Inertial Fusion
Osaka University, Osaka, Japan, March 10-14 1997

Abstract

This work describes a particular concept for ion induction linac accelerators using high-charge-state ions produced by an intense, short pulse laser, and compares the costs of a modular driver system producing 6.5 MJ for a variety of ion masses and charge states using a simple but consistent cost model.

1. Introduction and concept

The HIFSA study [1] found significant cost savings using heavy-ions of charge state q=3 relative to q=1, but further pursuit of high charge state ion designs was discouraged primarily because (a) beam transport costs in the low energy "front end" of the accelerator, which the HIFSA study had neglected, was expected to be expensive, (b) existing high-q ion sources, including laser-plasma sources [2], lacked sufficient charge-state purity, and (c), higher space charge with high-q ions would increase the minimum focal spot size or number of beams required in high-vacuum target chambers. Since the HIFSA study, PIC calculations [3] have shown that a few percent ionization of the low pressure background vapor ($\sim10^{-3}$ torr) present in an fusion chamber is sufficient to virtually eliminate the effects of beam space-charge on focal spot size.

The advent of intense, ultra-short-pulse lasers now suggests that specific high-ion charge states can be produced by multi-photon absorption at a controlled laser intensity, and with minimal collateral collisional ionization [4]. The laser-ion source concept schematically shown in Fig. 1 is proposed to address the issues (a) and (b) above. A frozen or liquid pellet of noble gas such as Argon or Xenon with the desired number of ions ($N_{io}\sim10^{14}$ to 10^{15} for a full-scale driver pulse) is first injected into a diode gap near the small anode end, when the injector voltage is initially off. A low energy laser pre-pulse shocks the 5 to 10 micron-radius pellet into a gas which is allowed to expand until a desired density (10^{-5} to 10^{-6} x critical density) is reached within the main laser focal spot. The initial density must be sufficiently low that recombination does not occur subsequent to the main laser pulse before the ions are extracted. An intense, ultra-short main laser pulse (~ 100 fs) then strips the ions down to a common ionization level by multi-photon absorption that is controlled by the laser intensity (10^{15} to 10^{17} W/cm^2 for ionization levels near 0.2 to 1 keV, depending on the laser wavelength and charge state). The diode voltage is then erected within 20 ns after the laser plasma begins to expand after the main laser pulse. Ions are extracted from the plasma sheath during expansion until the ion density is depleted.

The pulse length is proportional to the initial number of ions in the pellet, and inversely proportional to the space-charge-limited extraction current that is constrained by the diode gap size and voltage. The diode gap size is chosen so that the laser-plasma sheath expansion during the extraction pulse does not exceed 10% of the initial diode gap. A double solenoid is used to provide control over the shape and extent of the solenoid fringe field in the gap, so as to provide a matched Brillouin flow beam during the flat-top part of the diode voltage pulse.

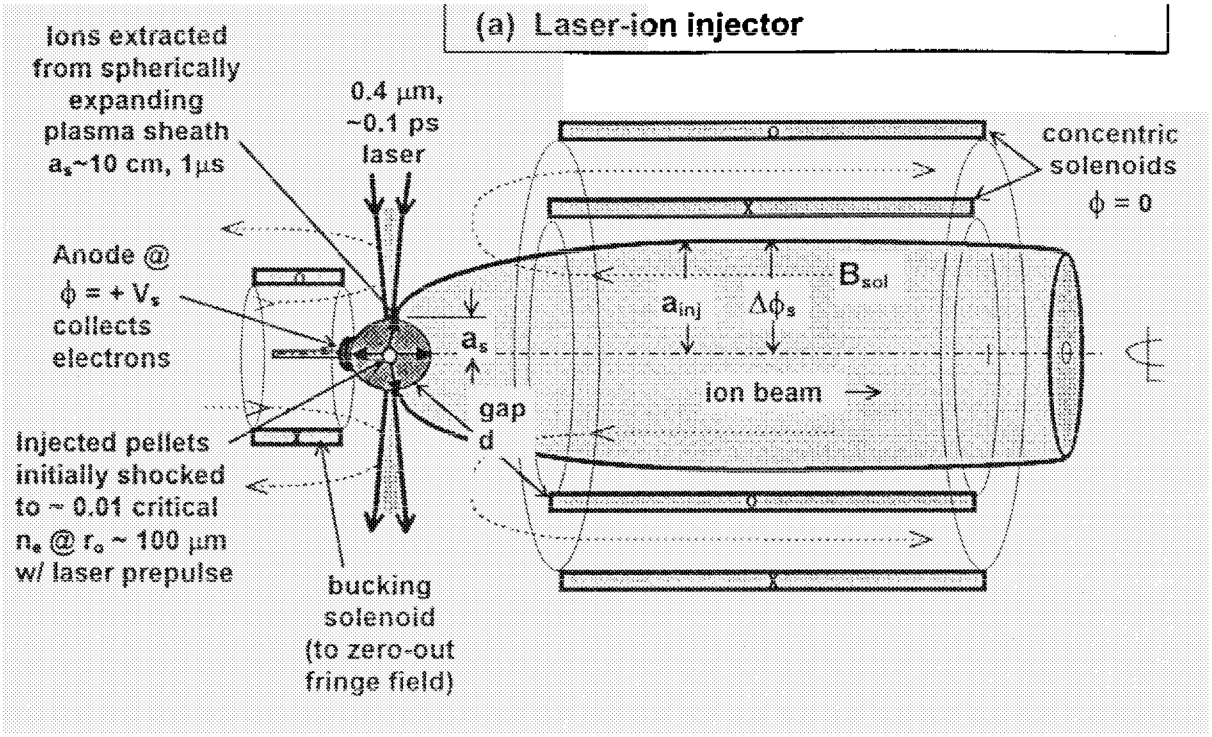
(a) Laser-ion injector

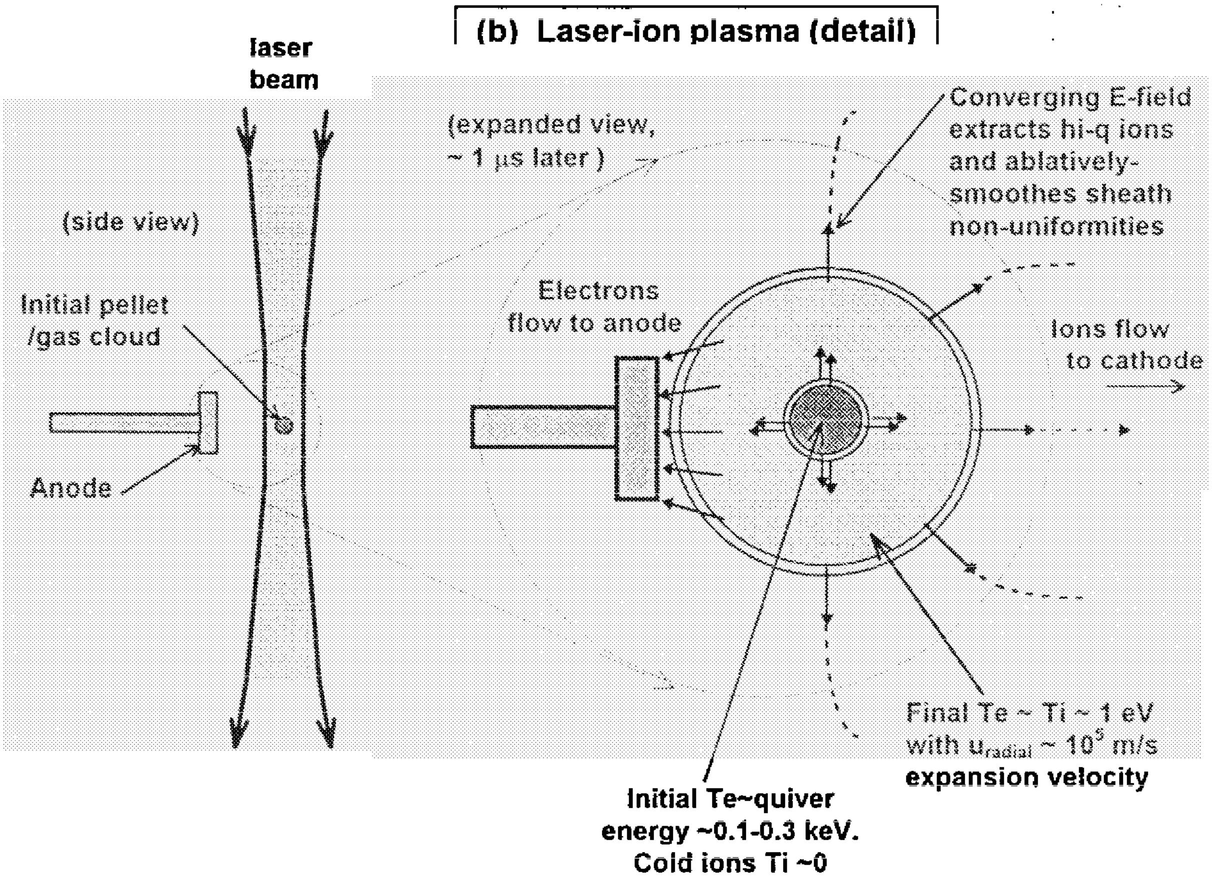
(b) Laser-ion plasma (detail)

Fig. 1 Concept for a high-charge-state ion source using ultra-short-pulse lasers.

According to applied-B diode theory [5], the strong solenoid magnetic field should prevent electrons field-emitted off the solenoid case from penetrating more than a few % distance into the diode gap. High breakdown gradients allowed at the cathode side, together with convergence of electric field lines on the small plasma anode sheath, and a space-charge-limited beam current proportional to $(q/A)^{1/2}$, are estimated to allow 100's of amperes extracted per source. With a sufficiently high ion q, say q = 8, and diode voltage $V_s = 3$ MV, ions would be injected with a sufficiently-high energy and velocity for economical magnetic transport with either solenoid or quadrupole focusing magnets, thus eliminating the need for a front-end with electrostatic-quadrupole focusing arrays and beam-merging.

The main issues to be addressed for this concept in future theory and experiment (beyond the scope of this paper) are: (1) ion charge state changes by three-body recombination and by charge-exchange with ions and neutrals, and (2) ion beam brightness and emittance with beam expansion and dynamic plasma sheath motion. Use of ionization levels just below a K or L-shell jump should prevent beam-beam charge exchange. If the ion-neutral charge-exchange cross section were 10^{-16} cm^2, a vacuum of 10^{-6} torr (10^{10} cm^{-3} neutral density) would give a mean-free path > 10 km, much longer than the linac lengths we will consider here. But if electron capture into highly excited states resulted in cx cross sections of say, 10^{-14} cm^2, a vacuum of 10^{-8} torr would be required.

For a given total beam energy at a given ion range required by a target, the accelerator voltage scales inversely with charge state q (reducing the length of a linac for a given limit on voltage gradient), but the voltage requirement for constant ion range also decreases with lower ion mass A (in AMU), and either way of reducing the accelerator voltage proportionately raises the total beam current (or number of beams) required for the same pulse length delivered to a target. Thus aside from the source issues (1) and (2), there is the question of how much a single driver cost might be reduced with a lower ion mass A at q=1 compared to using heavy ions at high q, assuming laser sources could provide any ion species. And aside from the cost of a single driver, there is another question of how much economic penalty is incurred if the larger number of beams required with higher q or lower A were subdivided into several identical linacs (modules), so that one module could validate the cost and performance (to reduce the development cost) of a modular driver system. The remainder of this paper addresses these latter questions concerning the potential use of high-charge-state ions.

2. Simplified cost model for modular high-q ion linacs

A simplified cost model [6] (too lengthy to reproduce here) has been developed for linacs using laser-ion sources, and with beam transport using either superconducting solenoid or quadrupole magnets. We have applied this model consistently to compare modular driver system costs for the matrix of ion masses A and charge states q that are listed in Table 1. Table 1 also gives the final ion kinetic energies Tf_{ion} required for a minimum ion range of 0.03 gm/cm^2 for high gain targets. The fourth and fifth charge states are chosen to be just below an L or K shell jump, to help insure charge-state purity. Note in Table 1 the ionization levels for the highest (fifth) charge states are all about 1 keV, requiring laser intensities ~ 10^{15} W/cm^2 at 0.4 micron wavelength.

Table 1 Ion species used for a comparative cost analysis of induction linac drivers.

Element	Mass A (AMU)	Z	1st q	2nd q	3rd q	4th q	5th q	5th E_i (eV)	Final Tf_{ion} (MeV)
Neon	20	10	1	2	4	8	10	1362	151
Argon	40	18	1	2	4	8	16	918	386
Krypton	84	36	1	2	4	8	26	1206	1120
Xenon	131	54	1	2	4	8	26	1013	2090

The key constraints and assumptions used in the model of ref. [6] are listed following:

1. The laser intensity for all cases is estimated for frequency-doubled Ti:sapphire (0.4 micron wavelength, 100 fs), and scales with the desired ionization level in each case.
2. The total ion beam energy and pulse length delivered to the target is 6.5 MJ and 10 ns, respectively, with final kinetic energies given in Table 1 for a constant range = 0.03 gm/cm^2.
3. The ion extraction pulse length is determined by a beam length out of the injector constrained to be less than 60 times the length on target (to have a common longitudinal spread allowance), together with a maximum laser plasma sheath expansion limited to 10 % of the diode gap.
4. The diode voltage V_s and current I_{inj} are calculated for a diode size consistent with (3) and conventional vacuum breakdown scaling (minimum diode voltages), and for higher diode gradients with magnetic insulation such that V_s = 10 MV (maximum diode voltage).
5. The total number of beams N_b and number of ions per source are calculated from (2) to (4).
6. The laser power and energy at 100 fs is determined by the initial gas target size to contain the required number of ions from (5), and the intensity required to produce the charge state.
7. Each ion case is evaluated and compared for transport with either superconducting solenoids or superconducting quadrupoles, operated at the same peak field at the windings of 3 T.
8. The beam length and average acceleration gradient V_g (1 MV/m) are both constant. The accelerator length with "load-and-fire" gives a final energy T_f *averaged* over beam length.
9. For the entire linac length, the beam radius a, transport magnet field and bore radius, and inner core radius, are all constant. The beam radius a is fixed at the beginning of the magnetic transport section to match the maximum transportable current at a coil occupancy factor η_o= 0.75. For solenoids, η is constant down the accelerator, while for quadrupoles, $\eta \sim \beta^{-1}$ as the beam accelerates. In addition, for quadrupole cases where the injection $\beta = v_z / c < 0.023$ (corresponding to 33 MeV Xenon), a low-cost ESQ array is inserted up to $\beta = 0.023$; to shrink the magnetic transport array size at the beginning of the magnetic transport section.
10. The number of beams per linac module is seven, so that the number of modules (# of linacs) N_m = integer(N_b / 7), plus one module for any remaining number of beams less than 7. This assumes flux return from each transport magnet is independent of adjacent beams (pessimistic).
11. Core losses are estimated as the volume of cores times 850 J/m^3, assuming an average pulse length of 1 microsecond, and 2.5 T flux swing. Pulser electrical efficiency is assumed to be 80 % based on all-solid state switching.

These simplifying assumptions allow analytic integral expressions to be evaluated for the costs of laser-ion sources at 10^5 \$/laser joule, beam transport with superconducting solenoids or quads at \$50 K/m of magnet, ferromagnetic core material at \$5/kg, pulsers at 10 \$/J, DC/cooling at 1.5 \$/W_e, and other (structure/insulators/cryo/vacuum/controls/buildings) at \$50 K/m of linac, for the various ion cases. For comparison purposes, relative costs are more useful than absolute costs with this simple model. Optimization of focusing magnet fields and core flux-swings as functions of z, combinations of solenoids in the front-end with more compact quads arrays in the high energy end, beam merging, etc., are all left for future work.

3. Results of the cost model

Table 2 lists the minimum and maximum diode voltages for the ion cases in Table 1, and Tables 3 through 8 list, for Table 1 ion cases and for minimum and maximum diode voltages, the injector currents per beam, the injector pulse lengths, the total number of beams required for 6.5 MJ, the accelerator lengths, the normalized total driver system direct costs with solenoid transport magnets, and the normalized driver costs with quadrupole transport magnets, respectively. Table 9 summarizes different Xenon driver cases, comparing both q =1 with q =26, for both single linac drivers and modular linac drivers. All driver system costs are normalized to a reference case of a single multi-beam linac for 6.5 MJ with q =1 Xenon ions, an ESQ front end, and 22 beams with magnetic quadrupole transport 2100 meters long for 2.1 GeV, for which the model predicts a direct cost of $ 1126 M.

Table 2 Minimum and maximum injector voltages V_s for laser-sources of ions given in Table 1.

	Minimum diode voltages (MV)					Maximum diode voltage (MV)				
Element	1st q	2nd q	3rd q	4th q	5th q	1st q	2nd q	3rd q	4th q	5th q
Neon	1.67	2.03	2.61	3.37	5.02	10	10	10	10	10
Argon	1.51	1.82	2.28	2.93	4.66	10	10	10	10	10
Krypton	1.44	1.72	2.17	2.77	5.04	10	10	10	10	10
Xenon	1.37	1.64	2.08	2.65	4.78	10	10	10	10	10

Table 3 Laser-source injector currents I_{inj} at minimum and maximum V_s, for Table 1 ion cases.

	I_{inj} (Amps) at minimum diode voltages					I_{inj} (Amps) at maximum diode voltage				
Element	1st q	2nd q	3rd q	4th q	5th q	1st q	2nd q	3rd q	4th q	5th q
Neon	20	38	79	164	333	297	420	594	839	938
Argon	12	23	46	94	267	210	297	420	594	839
Krypton	8	15	29	60	264	145	205	290	410	738
Xenon	6	11	22	45	195	116	164	232	328	591

Table 4 Injector pulse lengths τ_s at minimum and maximum V_s, for Table 1 ion cases.

	τ_s (μsec) at minimum diode voltages					τ_s (μsec) at maximum diode voltage				
Element	1st q	2nd q	3rd q	4th q	5th q	1st q	2nd q	3rd q	4th q	5th q
Neon	5.8	3.7	2.3	1.4	1.1	2.4	1.7	1.2	0.84	0.8
Argon	9.7	6.3	3.9	2.5	1.4	3.8	2.7	1.9	1.3	0.9
Krypton	16.9	10.9	6.9	4.3	1.8	6.4	4.5	3.2	2.3	1.3
Xenon	23.6	15.2	9.6	6.0	2.5	8.7	6.2	4.4	3.1	1.7

Table 5 Number of beams N_b for 6.5 MJ at minimum and maximum V_s, for Table 1 ion cases. The number of 7-beam linac modules N_m = integer(Nb / 7) plus one for any remaining beams.

	N_b at minimum diode voltages					N_b at maximum diode voltage				
Element	1st q	2nd q	3rd q	4th q	5th q	1st q	2nd q	3rd q	4th q	5th q
Neon	366	601	938	1450	1216	61	122	244	487	609
Argon	141	234	374	583	731	21	43	85	170	340
Krypton	44	73	116	181	323	6	13	25	50	163
Xenon	22	37	59	93	167	3	6	12	25	80

Table 6 Linac lengths L_a for 1 MV/m at minimum and maximum V_s, for Table 1 ion cases.

	L_a (m) at minimum diode voltages					L_a (m) at maximum diode voltage				
Element	1st q	2nd q	3rd q	4th q	5th q	1st q	2nd q	3rd q	4th q	5th q
Neon	161	85	47	39	34	153	77	35	27	23
Argon	397	204	107	58	44	388	196	99	41	35
Krypton	1131	572	292	152	55	1123	564	284	145	49
Xenon	2108	1061	538	275	92	2100	1053	530	268	87

Table 7 Normalized direct costs NDC [1 = \$1.126B] of modular 6.5 MJ driver systems at minimum and maximum V_s, for Table 1 ion cases, and for *solenoid* transport magnets.

	NDC at minimum diode voltages					NDC at maximum diode voltage				
Element	1st q	2nd q	3rd q	4th q	5th q	1st q	2nd q	3rd q	4th q	5th q
Neon	3.31	2.35	1.73	1.64	1.55	1.14	0.83	0.60	0.63	0.72
Argon	4.07	2.80	1.96	1.45	1.25	1.59	1.06	0.77	0.54	0.63
Krypton	5.00	3.33	2.21	1.51	0.96	2.10	1.37	0.96	0.71	0.56
Xenon	6.03	3.86	2.49	1.67	0.90	2.90	1.65	1.12	0.80	0.55

Table 8 Normalized direct costs NDC [1 = \$1.126B] of modular 6.5 MJ driver systems at minimum and maximum V_s, for Table 1 ion cases, and for *quadrupole* transport magnets.

	NDC at minimum diode voltages					NDC at maximum diode voltage				
Element	1st q	2nd q	3rd q	4th q	5th q	1st q	2nd q	3rd q	4th q	5th q
Neon	3.00	2.03	1.31	1.29	1.33	0.67	0.57	0.48	0.53	0.64
Argon	2.58	2.37	1.48	1.10	1.02	0.82	0.63	0.52	0.43	0.53
Krypton	2.23	1.96	1.71	1.05	0.79	1.12	0.68	0.56	0.48	0.46
Xenon	2.26	1.86	1.60	1.26	0.70	1.30	0.89	0.58	0.49	0.42

Table 9 Comparison of 6.5 MJ driver systems with minimum V_s, Xenon with 2.1 GeV final ion energy for 0.03 gm/cm^2 ion range in a target, and quadrupole transport magnets.

Parameter	Single linac (Xe^{+1})	Modular linacs (Xe^{+1})	Single linac (Xe^{+26})	Modular linacs (Xe^{+26})
# of beams (N_b)	22	22	167	167
# of linacs (N_m)	1	3 (7-beam) +1	1	23 (7-beam) +1
Length (m)	2108	2108	92	92
Core radius (m)	0.87	0.51	3.18	0.69
Efficiency (%)	33	16	72	46
Normalized cost	1	2.26	0.38	0.70

4. Conclusions

At this point many technical issues remain concerning the laser-ion-source concept shown in Fig.1 that will require detailed simulations and experiments to resolve, including high-q ion recombination and charge-exchange losses, limits on magnetized diode electric field gradient, extracted beam emittance from an expanding plasma sheath, longitudinal beam confinement and drift compression, and beam charge neutralization in the target chamber, to name a few. The question addressed here is: assuming laser-ion sources would work as modeled (or any equivalent high-q ion source), would there be sufficient potential benefits for a future driver, to justify the further R&D required for such sources? Based on different ion cases compared using a simple but consistently-applied cost model, the answer is: the potential benefits of high-q ion sources might be very large for drivers, and with important implications for the development cost of ion drivers. Quantitatively, this work suggests the potential benefits are: for single linac drivers, reduced driver cost (by 2.6 x) and increased efficiency (by 2.2 x), and for a modular driver system of linacs, by factors of 3.2 and 2.9, respectively. Most important, use of high-q ions for modular architectures might dramatically reduce the cost of an accelerator prototype which could both fully validate the performance of a driver, while providing significant capability for target physics experiments. If the simple cost model used here was to be trusted, one module of the Xe^{+26} system described in Table 9 would deliver 6.5 / 24 ~ 0.27 MJ of 2 GeV ions at a cost ~f x 0.7 x 1126 / 24 ~ \$ 33 M x f, where f is some cost multiplier > 1 for a one-of-a-kind prototype cost, as opposed to a mature driver system of modules. Conclusion? We should do more research on high-q ion sources.

*Work performed under the auspices of the US Department of Energy by Lawrence Livermore National Laboratory under Contract W-7405-Eng-48

References

[1] D. J. Dudziak, W. W. Saylor, and W. B. Herrmannsfeldt, "U.S. Heavy-Ion Fusion Systems Assessment Project Overview", Fusion Technology, Vol. 13, p. 207, Feb. 1988

[2] Laser and Particle Beams (1966), Vol. 14, No.3, see in particular, I. V. Roudsky "General features of highly charged ion generation in laser-produced plasmas", p. 369.

[3] D. A. Callahan, "Chamber propagation physics for heavy ion fusion", 7th Int. Symposium on Heavy-Ion Inertial Fusion, in Fusion Engineering and Design 32-33, (Nov. 1996), p.441

[4] M. D. Perry, A. Szoke, O. L. Landen, and E. M. Campbell, "Nonresonant Multiphoton Ionization of Noble Gases: Theory and Experiment", Phys. Rev. Letters, 60, No.13, Mar. 1988, p. 1270. See also M. D. Perry, et. al., Optical Society of Am. B, Vol.6, No. 3, Mar. 1989, p. 344

[5] M. P. Desjarlais, "Theory of Applied-B Ion Diodes", Phys. Fluids B 1(8), Aug. 1989, p.1709

[6] B. G. Logan, M. D. Perry, and G. J. Caporaso "Model for High-Charge-State Ion Induction Accelerators", Lawrence Livermore National Laboratory report UCRL-ID-126815, Feb. 1997.

Technical Information Department • **Lawrence Livermore National Laboratory**
University of California • Livermore, California 94551